NIH Public Access
Author Manuscript
J Neurophysiol. Author manuscript; available in PMC 2009 April 11.

Published in final edited form as:
J Neurophysiol. 2008 June ; 99(6): 3151–3156. doi:10.1152/jn.01031.2007.

Up-regulation of the T-type calcium current in small rat sensory neurons after chronic constrictive injury of the sciatic nerve

Miljen M. Jagodic[1], **Sriyani Pathirathna**[1], **Pavle M. Joksovic**[1], **WooYong Lee**[1,4], **Michael T. Nelson**[1,3], **Ajit K. Naik**[1], **Peihan Su**[1,3], **Vesna Jevtovic-Todorovic**[1,2,3], and **Slobodan M. Todorovic**[1,2,3]

1*Department of Anesthesiology, University of Virginia Health System, Charlottesville, VA 22908*

2*Department of Neuroscience, University of Virginia Health System, Charlottesville, VA 22908*

3*Department of Neuroscience Graduate Program, University of Virginia Health System, Charlottesville, VA 22908*

4*Department of Anesthesiology and Pain Medicine, InJe University, Sanggyepaik Hospital, Seoul, South Korea*

Abstract

Recent data indicate that peripheral T-type Ca^{2+} channels are instrumental in supporting acute pain transmission. However, the function of these channels in chronic pain processing is less clear. To address this issue, we studied the expression of T-type Ca^{2+} currents in small nociceptive dorsal root ganglion (DRG) cells from $L_{4\text{-}5}$ spinal ganglia of adult rats with neuropathic pain due to chronic constrictive injury (CCI) of the sciatic nerve. In control rats, whole-cell recordings revealed that T-type currents, measured in 10 mM Ba^{2+} as a charge carrier, were present in moderate density (20 ± 2 pA/pF). In rats with CCI, T-type current density (30 ± 3 pA/pF) was significantly increased, but voltage- and time-dependent activation and inactivation kinetics were not significantly different from those in controls. CCI-induced neuropathy did not significantly change the pharmacological sensitivity of T-type current in these cells to nickel. Collectively, our results indicate that CCI-induced neuropathy significantly increases T-type current expression in small DRG neurons. Our finding that T-type currents are up-regulated in a CCI model of peripheral neuropathy and earlier pharmacological and molecular studies suggest that T-type channels may be potentially useful therapeutic targets for the treatment of neuropathic pain associated with partial mechanical injury to the sciatic nerve.

Keywords

low-threshold-calcium channel; capsaicin; pain

INTRODUCTION

For more than two decades, it has been recognized that T-type (low-voltage-activated) Ca^{2+} channels (T-channels) have a key function in neuronal subthreshold membrane oscillations and spike firing in both the peripheral and central nervous system (reviewed in Perez-Reyes, 2003). However, the function of these channels in sensory and pain transmission (nociception) has only been discovered recently (Todorovic et al., 2001). New data have established the function of T-channels in supporting acute peripheral nociception. Furthermore,

Correspondence to Slobodan M. Todorovic Department of Anesthesiology, University of Virginia Health System, Mail Box 800710, Charlottesville, VA 22908-0710 Phone 434-924-2283, Fax 434-982-0019 Email:st9d@virginia.edu.

NIH-PA Author Manuscript
NIH-PA Author Manuscript
NIH-PA Author Manuscript

NIH-PA Author Manuscript

NIH-PA Author Manuscript

NIH-PA Author Manuscript

pharmacological and molecular down-regulation of the function these channels in DRG neurons also supports the notion that T-channels contribute to the chronic pain associated with peripheral axonal injury (reviewed in Jevtovic-Todorovic and Todorovic, 2006). However, in spite of the fact that T-type currents are expressed in several subpopulations of nociceptive DRG cells (Todorovic et al., 2001; Nelson et al., 2005; Coste et al., 2006), the cellular basis for the role of T-channels in chronic pain states is poorly understood. To address this issue, we used patch-clamp recordings to study the properties of T-type currents in acutely isolated and intact small nociceptive DRG neurons in animal model of painful peripheral neuropathy induced by chronic constrictive injury (CCI) of the sciatic nerve.

METHODS

Ethical approval was obtained for all experimental protocols from the University of Virginia Animal Care and Use Committee, Charlottesville, VA. All experiments were conducted in accordance with the *Guide for the Care and Use of Laboratory Animals* adopted by the U.S. National Institute of Health. Every effort was made to minimize animal suffering and the number of animals used.

Abnormalities in pain perception that are similar to those in humans, such as mechanical and thermal hyperalgesia, as well as mechanical allodynia, have been reported to occur in experimental rat models of mechanical injury of peripheral nerves as a consequence of loose ligation of the sciatic nerve, a chronic constrictive injury (CCI) (Bennett and Xie, 1988). We have published experimental procedures for CCI of the right sciatic nerve (Todorovic et al., 2004; Pathirathna et al., 2005) to induce mechanical injury to peripheral sensory nerve. For the present experiments, we used adult female retired-breeder Sprague-Dawley rats (250-350 gm, 6-10 months old). Control age-matched rats received either no operation (naïve animals) or sham operation (sham-operated animals). To determine the neuropathic state in CCI-treated rats, we measured thermal nociception in hind paws using thermal radiant heat testing as previously described (Todorovic et al., 2001; Todorovic et al., 2004; Pathirathna et al., 2005). For all behavioral data, we used analysis of variance (ANOVA) to compare the effects of CCI on thermal sensation. Subsequent pairwise comparisons between the pre- and post-CCI paw withdrawal latency (PWL) were done if significant P values resulted from two-way ANOVA. When appropriate, alpha levels were adjusted using the Bonferroni procedure (Pathirathna et al., 2005).

Before tissue harvest, rats were deeply anesthetized with isoflurane and rapidly decapitated. For one experiment, we dissected 2 dorsal root ganglia (DRGs), $L_{4\text{-}5}$ from ligated (right-side) from one CCI or sham-treated rat. In control (untreated, naive) rats, we used bilateral $L_{4\text{-}5}$ DRGs. We chose L_4 and L_5 DRGs since they contain the cell bodies of the majority of sensory fibers of the sciatic nerve. We prepared dissociated DRG cells and used them within 6-8 h for whole-cell recordings as previously described (Todorovic and Lingle, 1998). We focused only on small-size cells with an average soma diameter of 15-27 μm (Scroggs and Fox, 1992) since many functional studies have confirmed that the vast majority of them are nociceptors (Caterina and Julius, 2001; McCleskey and Gold, 1999).

Recordings were made according to the procedures we described previously, using standard whole-cell techniques with acutely dissociated DRG neurons (Todorovic and LIngle, 1998; Nelson et al., 2005; Jagodic et al., 2007; Nelson et al., 2007) and intact DRG neurons (Nelson et al., 2005). Series resistance (R_s) and capacitance (C_m) values were taken directly from readings of the amplifier after electronic subtraction of the capacitive transients. Series resistance was compensated to the maximum extent possible (usually ~60%-80%). In most experiments, we used a P/5 protocol for online leak subtractions.

NIH-PA Author Manuscript

NIH-PA Author Manuscript

NIH-PA Author Manuscript

Drugs were prepared as 100 mM stock solutions of $NiCl_2$ in H_2O. The external solution used to isolate Ca^{2+} currents contained, in mM, 10 $BaCl_2$, 152 TEA-Cl, and 10 HEPES adjusted to pH 7.4 with TEA-OH. To minimize contamination of T-type currents with even minimal HVA components, we used only fluoride (F^-)-based internal solution to facilitate high voltage-activated (HVA) Ca^{2+} current rundown; this solution contained (in mM) 135 tetramethyl-ammonium-hydroxide (TMA-OH), 10 EGTA, 40 HEPES, and 2 $MgCl_2$, adjusted to pH 7.2 with hydrofluoric acid (HF). This allowed studies of well-isolated and well-clamped T-type currents in acutely isolated DRG cells (Todorovic and Lingle, 1998). For voltage-clamp recordings with intact ganglia, the external solution contained the following (in mM): 140 NaCl, 4 KCl, 2 $MgCl_2$, 2 $CaCl_2$, 10 glucose, and 10 HEPES, adjusted to pH 7.4 with NaOH.; the pipette solution contained the following (in mM): 130 KCl, 5 $MgCl_2$, 1 EGTA, 40 HEPES, 2 Mg-ATP, and 0.1 Na-GTP, adjusted to pH 7.2 with KOH.

All chemicals were obtained from Sigma (St. Louis, MO) unless otherwise noted. Unless otherwise indicated, statistical comparisons were made, where appropriate, using an unpaired Student t-test, Mann-Whitney sum test, Signed rank test and chi-square test. All quantitative data are expressed as means of multiple experiments ± standard error of the mean (SEM). The percent reductions in peak current at various Ni^{2+} concentrations were used to generate a concentration-response curve. Mean values were fit to the following Hill function:

$$PB\left(\left[Ni^{2+}\right]\right) = PB_{max} / \left(1 + \left(IC_{50} / \left[Ni^{2+}\right]\right)^{n}\right) \quad (1)$$

where PB_{max} is the maximal percent block of peak current, IC_{50} is the concentration that produces 50% inhibition, and *n* is the apparent Hill coefficient for blockade. The fitted value is reported with 95% linear confidence limits. The voltage dependencies of activation and steady-state inactivation were described with single Boltzmann distributions of the following forms:

$$\text{Activation:} \quad G(V) = G_{max} / (1 + \exp[-(V - V_{50}) / K]) \quad (2)$$

$$\text{Inactivation:} \quad I(V) = I_{max} / (1 + \exp[(V - V_{50}) / k]) \quad (3)$$

In these forms, I_{max} is the maximal amplitude of current and G_{max} is the maximal conductance, V_{50} is the voltage where half of the current is activated or inactivated, and *k* represents the voltage dependence (slope) of the distribution. The amplitude of T-type current was measured from the peak, which was subtracted from the current at the end of the depolarizing test potential to avoid contamination with residual HVA currents that was present at more positive membrane potentials (typically −20 mV and higher).

RESULTS

Most of the rats developed a stable hyperesthetic state 5-7 days after being subjected to CCI of right sciatic nerve (Pathirathna et al., 2005). We confirmed the presence of CCI-induced thermal hyperalgesia before sacrifice (typically 7-14 days after CCI) for all animals used in voltage-clamp recordings. This was indicated by the reduction in thermal PWLs to 51.20 ± 0.01% of baseline values in right-side (ipsilateral, ligated) paws (n=34, $p < 0.001$). In contrast, thermal PWLs in these rats in left-side (contralateral, non-ligated) paws were not significantly affected: 99.80 ± 0.01% of baseline recorded before surgery (data not shown). Baseline values for PWLs were 10.47 ± 0.08 s in the right paws and 10.40 ± 0.08 s in the left paws. A sham

NIH-PA Author Manuscript

NIH-PA Author Manuscript

NIH-PA Author Manuscript

treatment did not significantly affect thermal PWLs up to 15 days after the procedure (data not shown).

We recorded from a total of 167 small-size acutely dissociated DRG cells. The average diameter of cell somas was (in μm): 24.2 ± 0.3 in the control group, 24.3 ± 0.2 in the CCI group, and 24.6 ± 0.9 in the sham group ($p > 0.05$). These included 77 cells from control naïve rats (n = 22 animals), 14 cells from sham-operated rats (n = 2 animals) and 76 cells from CCI-subjected rats (n = 34 animals).

To compare the expression of T-type voltage-gated Ca^{2+} currents in small DRG cells after the induction of CCI, we held cells at −90 mV, then imposed voltage commands of depolarizing pulses from −60 to 0 mV in 10-mV increments. A representative family of inactivating inward currents in small DRG cell from control and CCI-treated animals is depicted in Figure 1A and 1B, respectively. Note that in both cells T-type Ca^{2+} currents activate with small membrane depolarization, have a characteristic criss-crossing pattern, and display fast and almost complete inactivation during 250 ms-long test potentials. The average current-voltage curves were constructed from similar experiments, which indicated significant enhancement of T-type Ca^{2+} current amplitudes (measured from peak to the end of the depolarizing pulse) in CCI-treated animals; these currents were most prominent at negative membrane potentials and peaked at about −20 mV (Fig. 1C). To further determine the magnitude of the T-type current increase in CCI rats and to express it as current density, we normalized peak inward currents evoked at −30 mV to the cell capacitance in neurons from sham-operated, CCI-treated, and control rats. The histograms in Figure 1D indicate that T-type current density was enhanced about 1.5-fold in DRG cells from CCI rats as compared to cells from control ($p < 0.05$) and sham-operated rats ($p < 0.01$, Mann-Whitney test). Similarly, we found that the average T-current density in small DRG cells per rats had higher values in the CCI group (31.5 ± 4.2 pA/pF, n = 22 rats) than in the control group (20.6 ± 2.1 pA/pF, n = 16 rats, $p < 0.05$, Mann-Whitney test; data not shown). The average capacitance in these cells was (in pF): 19.4 ± 0.8 for the control group, 15.8 ± 0.7 for the CCI group ($p < 0.01$, t-test), and 19.3 ± 1.5 for the sham-operated group (data not shown). We also recorded T-currents from acutely isolated medium-size cells (n = 18) from CCI rats (n = 5) and found the following: average T-current density, 64 ± 12 pA/pF; average cell soma diameter, 33.8 ± 4.4 μm, average cell capacitance, 31.4 ± 2.7 pF; data not shown). None of these parameters was statistically different from those for medium DRG cells in control rats recorded under identical experimental conditions (Jagodic et al., 2007). Next, we used data presented in Fig. 1D to generate linear correlation curves from scatter plots of T-type current density against cell capacitance in control and CCI groups. We found significant correlation only in the CCI group ($p < 0.001$), not in the control one ($p = 0.2$, data not shown). These data suggest that CCI-induced increase in T-type current density occurred predominantly in the subpopulation of smallest DRG cells.

We also measured time-dependent activation (10%-90% rise time, Fig. 1E) and time-dependent inactivation time constants (τ) (single exponential fit of decaying portion of the current waveforms, Fig. 1F) from current-voltage curves in these cells over the range of test potentials from −50 mV to 0 mV. We found a small but significant difference between the controls and CCI-treated groups only for inactivation τ at 0 mV (Fig. 1F). The proportion of cells expressing T-type current was not significantly different in these two groups: control, 69% and CCI, 70% (χ-square test, data not shown).

We also tested voltage-dependent (steady-state) inactivation, finding that CCI caused a very small depolarizing shift in the midpoint (V_{50}) of inactivation in these cells. For example, Figure 2B shows that the inactivation, V_{50}, was about −69 mV in control cells (n = 13) and −66 mV in DRG cells from CCI-induced neuropathic rats (n = 17) ($p > 0.05$). Likewise, the average V_{50} for T-type channel activation calculated from current-voltage curves was not significantly

NIH-PA Author Manuscript

NIH-PA Author Manuscript

NIH-PA Author Manuscript

different in cells from the control (−42 mV, n = 15) and CCI (−41 mV, n = 24) groups (Fig. 2C). In contrast, we recently reported up-regulation and a depolarizing shift in voltage-dependent inactivation of T-type channels in a subpopulation of medium-size DRG cells in rats with streptozotocin-induced diabetic neuropathy (Jagodic et al., 2007). Thus, it appears that diabetic and mechanical neuropathy may affect T-type channels differently in different subpopulations of DRG cells.

Previous data using in-situ hybridization (Talley at al., 1999), knock-out (Chen et al., 2003), and molecular knock-down (Bourinet et al., 2005) have established that $Ca_V3.2$ is a predominant isoform of T-type channels in small DRG nociceptors from normal rats. Thus, we examined the pharmacological properties of these cells in a CCI model of peripheral neuropathy, testing their sensitivity to nickel, a $Ca_V3.2$-specific pharmacological tool that is a traditional T-type channel blocker (Lee et al., 1999). Figure 3A shows representative traces and Figure 3B shows representative time courses from experiments in which nickel reversibly blocked T-type current in a concentration-dependent manner at 10 and 30 μM. However, when we compared IC_{50} for nickel in control cells (about 29 μM, n = 4 cells) versus DRG cells from CCI-treated rats (about 34 μM, n = 7 cells) there was very little difference between the two groups (Fig. 3C). There was no significant difference between cells in the control and CCI group with respect to the amplitude of T-type current blocked by 10, 30 and 100 μM nickel. For example, 30 μM nickel blocked 42.5 ± 4.5 % T-type current in DRG cells from CCI rats (n = 4), and 50 ± 5% in DRG cells from control rats ($p > 0.05$). The fact that pharmacological sensitivity to nickel is very similar in both cells from CCI rats and control cells, together with the minimal changes in channel kinetics, strongly suggest that the molecular composition of T-type currents is little affected in small DRG cells from CCI-subjected rats.

Next, we performed experiments to estimate the contribution of T-type current to cellular excitability in these cells. In order to provide more physiologically relevant data, we performed these recordings using small cells in intact L_{4-5} DRGs (Nelson et al., 2005) and measured peak inward currents evoked from V_h −90 mV in 5-mV increments. We reasoned that voltage for half-maximal activation of total voltage-gated inward currents in these cells may be shifted to more depolarized potentials in the presence of 100 μM nickel. Indeed, Figure 3D shows that nickel significantly increased the half-maximal activation threshold from −40±1 mV to −31±3 mV ($p < 0.01$; n = 11 cells from 4 rats) in CCI, but not in DRG cells from sham-operated rats (baseline: −37 ± 3 mV, nickel −36 ± 3 mV; $p > 0.05$; n = 8 cells from 3 rats). Interestingly, there was no significant difference in baseline half-threshold activation in the two groups. This could be explained by the concomitant decrease in TTX-resistant Na^+ current density reported previously in small DRG cells in rats with CCI (Dib-Hajj et al., 1999). TTX-resistant Na^+ channels activate over a range of potentials similar to that which activates T-type channels and are often co-expressed in the same DRG cells (Coste et al., 2007).

DISCUSSION

Here we demonstrate that CCI of the sciatic nerve induces up-regulation of $Ca_V3.2$ T-type Ca^{2+} currents in small DRG neurons, most of which likely represent the cell somas of classically described peripheral nociceptors. In vitro, these cells express functional properties of nociceptors such as responses to capsaicin-, heat-, proton- and ATP-gated currents (Todorovic et al., 2001), as well as high-threshold mechano-sensory currents (Coste et al., 2007). Thus, it is very likely that these T-channel-containing small DRG cells are polymodal nociceptors capable of responding in vivo to noxious heat, chemical, and mechanical stimuli. Recent data indicate that T-type channels have an important function in enhancing the cellular excitability of at least some small DRG cells by reducing the threshold for action potential firing (Nelson et al., 2005) and contributing to Ca^{2+} entry during action potentials (Blaire and Bean, 2002; Nelson et al., 2005). In spite of their modest expression in most small DRG cells,

NIH-PA Author Manuscript

NIH-PA Author Manuscript

NIH-PA Author Manuscript

increased T-type current density similar to that described here in our CCI model could be sufficient to increase the probability of the firing of action potentials, since these cells have high-input resistance, as we have directly demonstrated in our current clamp recordings using T-type channel modulators and $Ca_V3.2$ knock-out mice (Nelson et al, 2007).

It is important to note that remodeling of other voltage- and ligand-gated ion channels that can alter the excitability of the sensory neurons has been proposed to have a critical function in the development and maintenance of neuropathic pain symptoms such as hyperalgesia and allodynia (Woolf 2004; Campbell and Meyer, 2006). Thus, it is unlikely that changes in T-type current expression in the CCI model are the only culprit, but may contribute to complex plasticity and to overall alteration in the cellular excitability of injured sensory neurons. In a simple model of measure of cellular excitability, we found that nickel at concentrations thought to be selective for T-type current significantly lowered the threshold for half-maximal activation of total inward current largely carried by voltage-gated Na^+ channels in these cells from CCI-subjected but not sham-operated rats. These data suggest that up-regulated T-type currents may have a more prominent part in lowering threshold for spike firing in small DRG cells from CCI rats than in healthy rats.

Unlike pain that is caused by acute tissue injury (nociceptive pain), neuropathic pain resulting from constrictive nerve damage is a debilitating disorder that is inconsistently responsive to currently available conventional treatments. Of particular interest is our finding that several pharmacological blockers and modulators of T-type channels in vivo alleviate neuropathic pain in CCI. We determined that a series of 5α-reduced neuroactive steroids (e.g., (+)-ECN) are potent and selective blockers of DRG T-type channels in vitro (Todorovic et al., 1998). Furthermore, consistent with our present findings, (+)-ECN had a more potent analgesic effect when injected locally in peripheral receptive fields of sensory neurons in rats with CCI than it did when injected in control rats (Pathirathna et al., 2005). Dogrul and colleagues (2003) found that the preferential T-type channel blockers mibefradil and ethosuximide effectively reverse hyperalgesia and allodynia from CCI. We also found that oxidizing agents that block DRG T-type channel in vitro are capable of reversing CCI-induced thermal hyperalgesia in vivo (Todorovic et al., 2004). Moreover, application of the T-type channel blocker Ni^{2+} blocks ectopic discharges from peripheral nerves in a model of segmental spinal mechanical injury (Liu et al., 2001). Toward this end, specific molecular silencing of $Ca_V3.2$ T-type channels in DRG cells with antisense reverses both hyperalgesia and allodynia in rats with CCI (Bourinet et al., 2005).

Surprisingly, in-vivo study using $Ca_V3.2$ knock- out mice did not find a difference in pain perception in a CCI model (Choi et al., 2006). The exact reason for this discrepancy is not known, but it is possible that developmental elimination of $Ca_V3.2$ channels allows compensatory changes that are not feasible during acute down-regulation of channel function using pharmacological agents or antisense applications. Interestingly, previous patch-clamp recordings of DRG Ca^{2+} channels in CCI also gave contrasting results. Hogan et al. (2000) reported no change in total inward Ca^{2+} currents in small DRG cells, and loss of T-type current in medium-size DRG cells in rats with CCI (McCallum et al., 2003). These authors also reported that in control animals they did not observe T-type currents in any small DRG cells (< 29 μm soma diameter). This is in sharp contrast to the results of this and previous studies (Todorovic and Lingle, 1998; Todorovic et al., 2001; Scroggs and Fox, 1992; Cardenas et al., 1995; Coste at all, 2007; Blaire and Bean, 2002), which found that T-type currents are expressed in the majority of small DRG nociceptors, and that T-type current in medium-size DRG cells is not affected with peripheral nerve injury (Baccei and Kocsis, 2000). Thus, it is possible that different experimental conditions or the selection of different cells can account for the different findings with regard to the effect of CCI on expression of Ca^{2+} channels in small and medium DRG cells.

NIH-PA Author Manuscript

NIH-PA Author Manuscript

NIH-PA Author Manuscript

Our present study further implicates T-type channels as possible targets for the treatment of neuropathic pain resulting from mechanical injury to peripheral axons of sensory neurons. Thus, blocking T-type channels may offer new therapeutic options for alleviating patients' suffering from chronic intractable pain resulting from partial mechanical injury of peripheral nerves. Future studies must be focused on the mechanisms of T-type channel alterations in these cells by CCI and in other animal models of painful neuropathy.

Acknowledgments

Supported in part by NIGMS R01 075229 grant and funds from Department of Anesthesiology at UVA to S.M.T. and funds from Dr. Harold Carron endowment to V.J-T.

REFERENCE LIST

Baccei ML, Kocsis JD. Voltage-gated calcium currents in axotomized adult rat cutaneous afferent neurons. J Neurophysiol 2000;83(4):2227–2238. [PubMed: 10758131]

Blair NT, Bean BP. Roles of tetrodotoxin (TTX)-sensitive Na+ current, TTX-resistant Na+ current, and Ca2+ current in the action potentials of nociceptive sensory neurons. J Neurosci 2002;22:10277–90. [PubMed: 12451128]

Bennett GJ, Xie YK. A peripheral mononeuropathy in rat that produces disorders of pain sensation like those seen in man. Pain 1988;33:87–107. [PubMed: 2837713]

Bourinet E, Alloui A, Monteiol A, Barrere C, Couette B, Poirot O, Pages A, McRory J, Snutch TP, Eschalier A, Nargeot J. Silencing of the $Ca_V3.2$ T-type calcium channel gene in sensory neurons demonstrates its major role in nociception. EMBO J 2005;24:315–324. [PubMed: 15616581]

Campbell JN, Meyer RA. Mechanisms of neuropathic pain. Neuron 2006;52:77–92. [PubMed: 17015228]

Cardens CG, Del Mar LP, Scroggs RS. Variation in serotonergic inhibition of calcium channel currents in four types of rat sensory neurons differentiated by membrane properties. J Neurophysiol 1995;74:1870–1879. [PubMed: 8592180]

Caterina MJ, Julius D. The vanilloid receptor: a molecular gateway to the pain pathway. Ann Rev Neurosci 2001;24:487–517. [PubMed: 11283319]

Chen CC, Lamping KG, Nuno DW, Barresi R, Prouty SJ, Lavoie JL, Cribbs LL, England SK, Sigmund CD, Weiss RM, Williamson RA, Hill JA, Campbell KP. Abnormal coronary function in mice deficient in alpha1H T-type Ca2+ channels. Science 2003;302:1416–8. [PubMed: 14631046]

Choi S, Na HS, Kim J, Lee J, Lee S, Kim D, Park J, Chen CC, Campbell KP, Shin HS. Attenuated pain responses in mice lacking CaV3.2 T-type channels. Genes Brain Behav 2007;6(5):425–431. [PubMed: 16939637]

Coste B, Crest M, Delmas P. Pharmacological dissection and distribution of NaN/Nav1.9, T-type Ca2+ currents, and mechanically activated cation currents in different populations of DRG neurons. J Gen Physiol 2007;129(1):57–77. [PubMed: 17190903]

Dib-Hajj SD, Fjell J, Cummins TR, Zheng Z, Fried K, LaMotte R, Black JA, Waxman SG. Plasticity of sodium channel expression in DRG neurons in the chronic constriction injury model of neuropathic pain. Pain 1999;83(3):591–600. [PubMed: 10568868]

Dogrul A, Gardell LR, Ossipov MH, Tulunay FC, Lai J, Porecca F. Reversal of experimental neuropathic pain by T-type calcium channel blockers. Pain 2003;105:159–168. [PubMed: 14499432]

Hogan QH, McCallum JB, Sarantopoulos C, Aason M, Mynlieff M, Kwok WM, Bosnjak ZJ. Painful neuropathy decreases membrane calcium current in mammalian primary afferent neurons. Pain 2000;86(12):43–53. [PubMed: 10779659]

Jagodic MM, Pathirathna S, Nelson MT, Mancuso S, Joksovic PM, Rosenberg ER, Bayliss DA, Jevtovic-Todorovic V, Todorovic SM. Cell-specific alterations of T-type calcium current in painful diabetic neuropathy enhance excitability of sensory neurons. J Neurosci 2007;21:27(12):3305–16. [PubMed: 17376991]

Jevtovic-Todorovic V, Todorovic SM. The role of peripheral T-type calcium channels in pain transmission. Cell Calcium 2006;40(2):197–203. [PubMed: 16777222]

NIH-PA Author Manuscript

NIH-PA Author Manuscript

NIH-PA Author Manuscript

Lee JH, Gomora JC, Cribbs LL, Perez-Reyes E. Nickel block of three cloned T-type calcium channels: low concentrations selectively block alpha1H. Biophys J 1999;77(6):3034–42. [PubMed: 10585925]

Liu X, Zhou J-L, Chung K, Chung JM. Ion channels associated with the ectopic discharges generated after segmental spinal nerve injury in the rat. Brain 2001;900:119–127.

McCallum JB, Kwok WM, Mynlieff M, Bosnjak ZJ, Hogan QH. Loss of T-type calcium current in sensory neurons of rats with neuropathic pain. Anesthesiology 2003;98(1):209–16. [PubMed: 12502999]

McCleskey EW, Gold MS. Ion channels of nociception. Ann Rev Physiol 1999;61:835–856. [PubMed: 10099712]

Nelson MT, Joksovic PM, Perez-Reyes E, Todorovic SM. The endogenous redox agent L-cysteine induces T-type Ca^{2+} channel-dependent sensitization of a novel subpopulation of rat peripheral nociceptors. J Neurosci 2005;25(38):8766–75. [PubMed: 16177046]

Nelson MT, Woo J, Kang H-W, Barrett PQ, Vitko J, Perez-Reyes E, Lee J-H, Shin H-S, Todorovic SM. Reducing agents sensitize C-type nociceptors by relieving high-affinity zinc inhibition of T-type calcium channels. J Neurosci 2007;27(31):8250–8260. [PubMed: 17670971]

Perez-Reyes E. Molecular physiology of low-voltage-activated T-type calcium channels. Physiol Rev 2003;83:117–161. [PubMed: 12506128]

Pathirathna S, Todorovic SM, Covey DF, Jevtovic-Todorovic V. Novel 5α-reduced neuroactive steroids induce peripheral thermal anti-nociception in rats with neuropathic pain. Pain 2005;117(3):326–339. [PubMed: 16150542]

Scroggs RS, Fox AP. Calcium current variation between acutely isolated adult rat dorsal root ganglion neurons of different size. J Physiol (Lond) 1992;445:639–658. [PubMed: 1323671]

Talley EM, Cribbs LL, Lee JH, Daud A, Perez-Reyes E, Bayliss DA. Differential distribution of three members of a gene family encoding low voltage-activated (T-type) calcium channels. J Neurosci 1999;19:1895–1911. [PubMed: 10066243]

Todorovic SM, Lingle CJ. Pharmacological properties of T-type Ca^{2+} current in adult rat sensory neurons: effects of anticonvulsant and anesthetic agents. J Neurophysiol 1998;79:240–252. [PubMed: 9425195]

Todorovic SM, Prakriya M, Nakashima YM, Nillson KR, Han M, Zorumski CF, Covey DF, Lingle CJ. Enantioselective blockade of T-type Ca^{2+} current in adult rat sensory neurons by a steroid that lacks GABA-modulatory activity. Mol Pharmacol 1998;54:918–927. [PubMed: 9804627]

Todorovic SM, Jevtovic-Todorovic V, Meyenburg A, Mennerick S, Perez-Reyes E, Romano C, Olney JW, Zorumski CF. Redox modulation of T-type calcium channels in rat peripheral nociceptors. Neuron 2001;31:75–85. [PubMed: 11498052]

Todorovic SM, Meyenburg A, Jevtovic-Todorovic V. Redox modulation of peripheral T-type Ca^{2+} channels in vivo: alteration of nerve injury-induced thermal hyperalgesia. Pain 2004;109:328–339. [PubMed: 15157694]

Woolf CJ. Dissecting out mechanisms responsible for peripheral neuropathic pain: implications for diagnosis and therapy. Life Sci 2004;74(21):2605–10. [PubMed: 15041442]

NIH-PA Author Manuscript
NIH-PA Author Manuscript
NIH-PA Author Manuscript

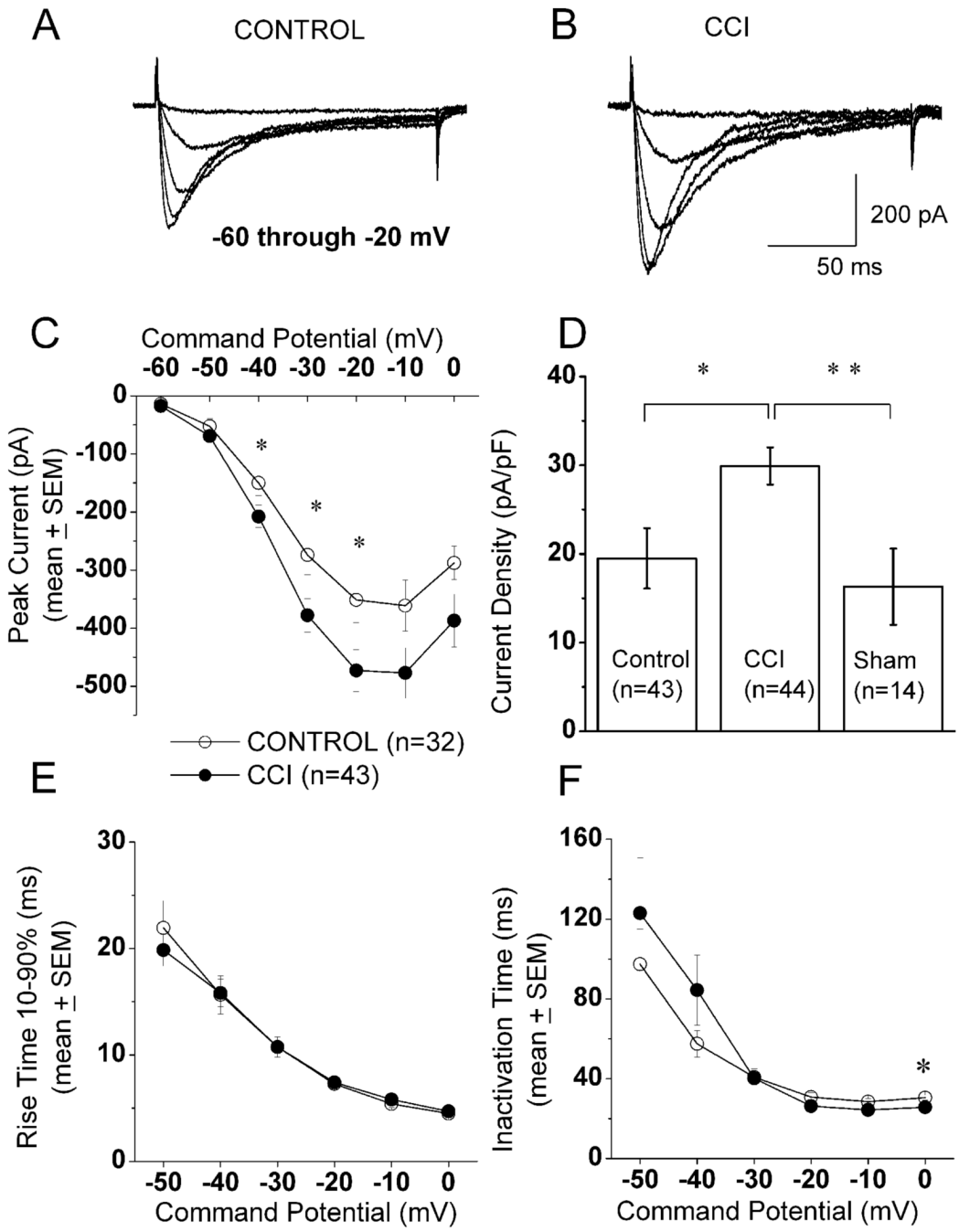

Figure 1. Up-regulation of T-type current in small DRG cells following CCI

A,B: Traces represent families of inward Ca^{2+} currents evoked in representative small DRG cells from control (panel A: Cm 17.6 pF, R_s 1.3 MΩ) and CCI-subjected rats (panel B: Cm 25.3 pF, R_s 1.0 MΩ) by voltage steps from −90 mV (V_h) to V_t from −60 through −20 mV in 10-mV increments. Traces are leak subtracted and averaged from 3 consecutive sweeps. Calibration bars pertain to both panels.

C: Average current-voltage curves from similar experiments as depicted in panels A and B are representative of control (open symbols) and CCI (black symbols) small-size DRG cells. CCI more prominently increased the absolute average amplitude of inward Ca^{2+} current at negative test potentials. For example, at V_t −30 mV, average control peak current was −274 ± 34 pA,

NIH-PA Author Manuscript

NIH-PA Author Manuscript

NIH-PA Author Manuscript

while average peak in CCI group was −378 ± 29 pA ($p<0.05$); Vertical bars indicate ± SEM of multiple determinations. The amplitude of the total inward current at any given potential was measured from the end of the pulse to its peak. Asterisks indicate significance ($p < 0.05$ or higher) by t-test or Mann-Whitney U test. The numbers in parentheses indicate the number of cells in samples.

D: Histograms indicate average T-type current amplitudes in small DRG cells from control, sham-operated and CCI-subjected rats expressed as current density in pA/pF to correct for differences in cell size. Amplitude of T-type current was measured as maximal peak current subtracted from the small sustained current at the end of the depolarizing pulse at V_t −30 mV. Size of each sample is in the parenthesis; vertical bars are SEM of multiple determinations. Peak T-type current density averaged 20 ± 2 pA/pF in the control, 30 ± 3 pA/pF in the CCI group and in sham group averaged 16 ± 4 pA/pF. ** indicates significant value by Mann-Whitney test ($p < 0.01$); * indicates significant value by Mann-Whitney test ($p < 0.05$);

E,F: We measured time-dependent activation (10%-90% rise time, panel E) and inactivation τ (single exponential fit of decaying portion of the current waveforms, panel F) from current-voltage curves in these cells over the range of test potentials from −50 mV to 0 mV. We found very little differences between the control and CCI groups. Note that both activation and inactivation show acceleration and eventually voltage-independent process at more positive potentials. * $p<0.05$

NIH-PA Author Manuscript

NIH-PA Author Manuscript

NIH-PA Author Manuscript

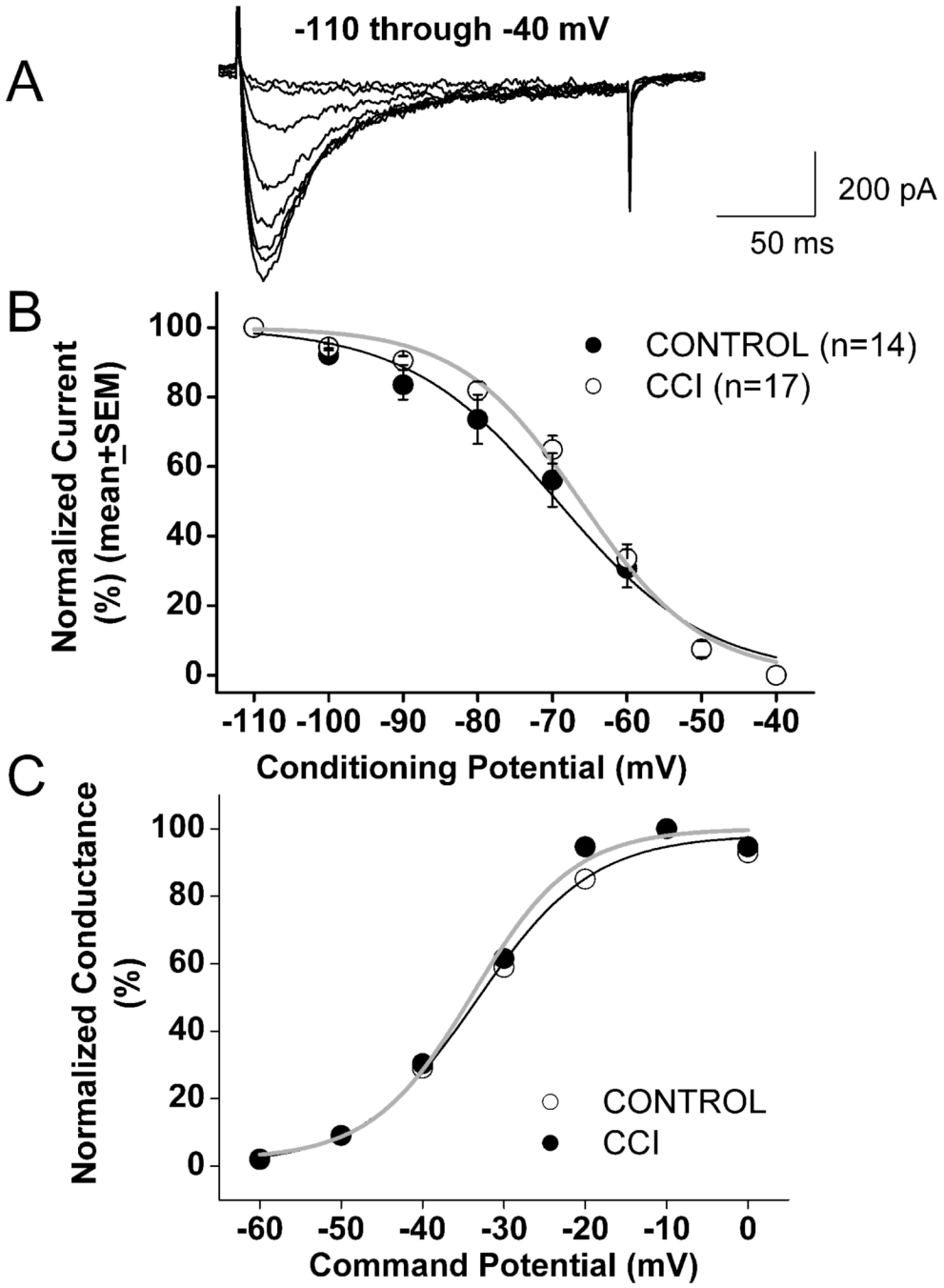

Figure 2. Voltage-dependent kinetic properties of T-type currents in CCI-treated rats

A: Representative raw current traces the DRG cells from CCI-treated rat (C_m 20 pF, R_s 1.0 MΩ). Currents are evoked by test steps to −30 mV after a 3.5-s prepulse at potentials from −110 mV to −40 mV in 10 mV increments.

B: Normalized peak T-type current steady-state curves for voltage-dependent inactivation from similar experiments depicted in upper panel of this figure. All points are averages from different cells as noted in parentheses: open symbols represent the control group; filled black symbols represent the CCI group. Verticals lines are SEM of multiple determinations. Solid lines are fitted using equation #3, giving half-maximal availability (V_{50}) that occurred at −69.3 ± 1.1 mV with a *k* of 10 ± 1 mV in the control group (black line). V_{50} was −66.2 ± 0.9 mV with a

NIH-PA Author Manuscript

NIH-PA Author Manuscript

NIH-PA Author Manuscript

k of 8 ± 1 mV in the CCI group (gray line). Note a parallel shift to the right of the average fit in CCI cells.

C: These curves show apparent peak conductance values defined as $I_{peak}/(V-E_r)$ plotted against command potentials in whole-cell recordings from control (open symbols) and CCI (filled symbols) cells calculated from the average current-voltage curve depicted in Figure 1C. The extrapolated reversal potential (E_r) was taken to be + 60 mV and was calculated in cells in which maximal HVA current amplitude was not bigger than T-type current amplitude by running 10 mV incremental depolarizing steps from −60 to +60 mV. Solid lines are fitted using equation #2, giving half-maximal conductance (V_{50}) that occurred at −33.3 ± 1.4 mV with a *k* of 7.1 ± 1.4 mV in the control group (black line) and V_{50} was −33.8 ± 1.4 mV with a *k* of 6.2 ± 1.3 mV in the CCI group (gray line).

NIH-PA Author Manuscript
NIH-PA Author Manuscript
NIH-PA Author Manuscript

Figure 3

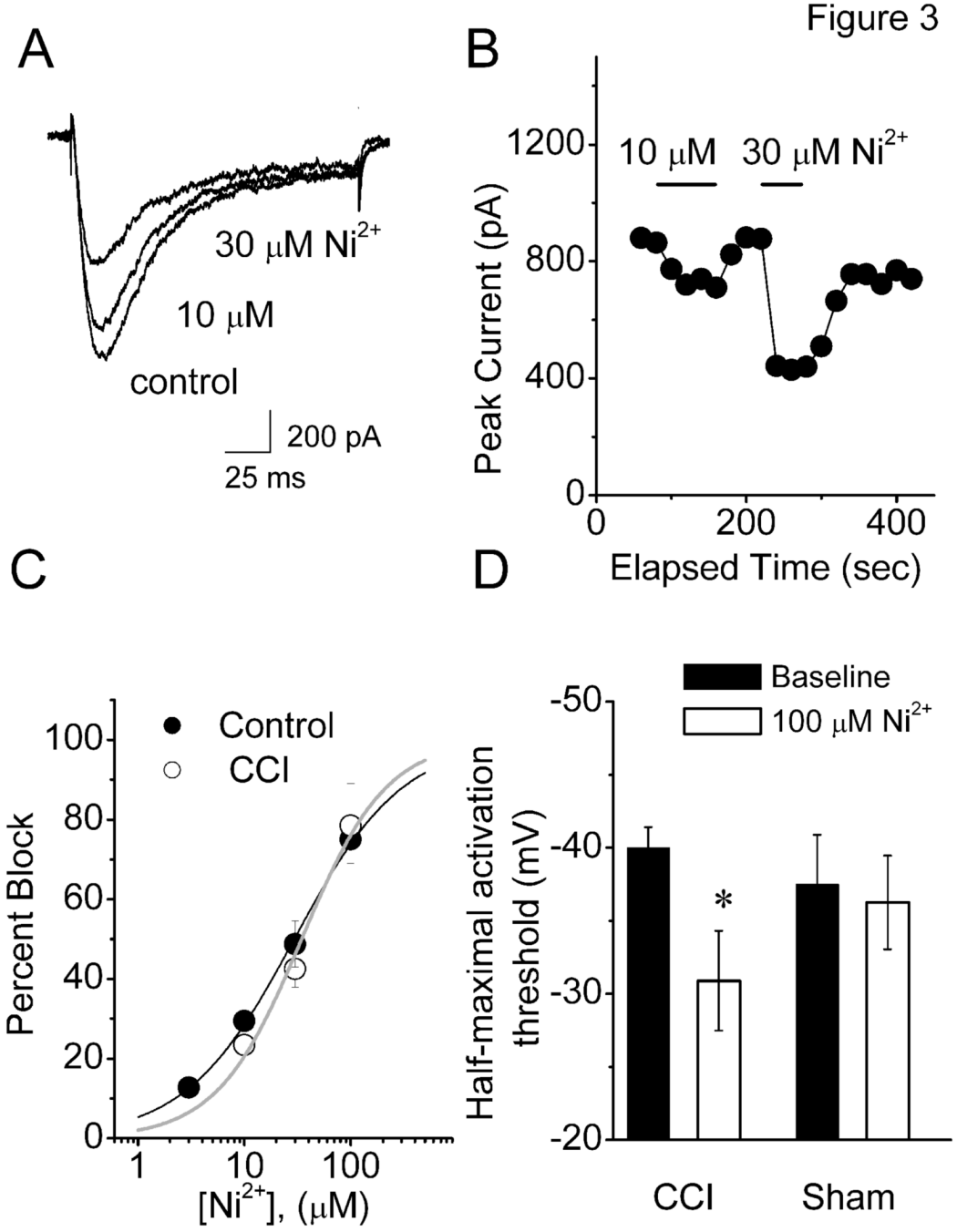

Figure 3. Nickel blocks DRG T-type current in CCI and control groups with similar potency

A. Representative T-type current traces showing concentration-dependent block with escalating concentrations (10 and 30 μM) of Ni^{2+} in small-size DRG cell from the rat subjected to CCI (C_m 19.4 pF; R_s 1.3 MΩ). Bars indicate calibration.

B. Time course of the effects of different concentrations of Ni^{2+} on the peak T-type current from the same experiment presented on panel A of this figure. Horizontal bars indicate the time of drug applications. Note rapid onset and reversal of the effects of nickel on the peak T-type current.

C. Concentration-response curves from multiple experiments showing block of T-type current by Ni^{2+} in control (filled symbols) and CCI (open symbols) small-size DRG cells. Every

NIH-PA Author Manuscript

NIH-PA Author Manuscript

NIH-PA Author Manuscript

symbol represents averages from multiple cells (4 control and 7 in CCI); vertical lines are ± SEM. Solid lines are best fits obtained in controls (black line) using equation #1, which gave IC_{50} of 29.4 ± 1.4 μM, and n of 0.85 ± 0.04 and; in CCI cells (gray line), IC_{50} of 34.5 ± 4.8 μM and n of 1.09 ± 0.18. Both fits are constrained to 100% maximal block.

D. Histograms demonstrate that nickel diminished cellular excitability in small cells from intact L_{4-5} DRGs in rats with CCI but not sham-operated rats. Half-maximal activation threshold for total inward currents was significantly increased in CCI group after application of 100 μM nickel (blank column) relative to baseline values obtained before nickel application (filled columns). * p=0.002, Signed rank test